Aerosol Optical Depth retrievals in Central Amazonia from a Multi-Filter Rotating Shadow-band Radiometer on-site calibrated

Nilton E. Rosário[1], Tamara Sauini[1], Theotonio Pauliquevis[1], Henrique M. J. Barbosa[2], Marcia A. Yamasoe[3], Boris Barja[4]

[1]Universidade Federal de São Paulo - Rua São Nicolau 210 - Diadema - SP - CEP 09913-030 – Brazil

[2]Instituto de Física da Universidade de São Paulo - Rua do Matão 1371 - São Paulo - SP - CEP 05508-090 - Brazil

[3]Instituto de Astronomia, Geofísica e Ciências Atmosféricas - Universidade de São Paulo - Rua do Matão 1226 - São Paulo - SP - CEP 05508-090 – Brazil

[4]Universidade de Magallanes - Manuel Bulnes 01855, Punta Arenas, Region de Magallanes y de la Antártica Chilena, Chile

Correspondence to: Nilton E. Rosario (nrosario@unifesp.br)

Abstract

Extraterrestrial spectral response calibration of a Multi-Filter Rotating Shadow band Radiometer (MFRSR) under Amazonian Forest atmosphere pristine conditions using the Langley plot method was performed and evaluated. The MFRSR is installed in Central Amazonia as part of a long-term monitoring site, which was used in the context of the GoAmazon2014/5 Experiment. It has been operating continuously since 2011 without regular extraterrestrial calibration, preventing its application to accurate monitoring of aerosol particles. Once calibrated, the MFRSR measurements were applied to retrieve aerosol particles columnar optical properties, specifically Aerosol Optical Depth (AOD_{λ}) and Ångström Exponent (AE), which were evaluated against retrievals from a collocated CIMEL sunphotometer belonging to the AErosol RObotic NETwork (AERONET). Results obtained revealed that Amazonian pristine conditions are able to provide MFRSR extraterrestrial spectral response with relative uncertainty lower than 1.0% at visible channels. The worst estimate (air mass = 1) for absolute uncertainty in AOD_{λ} retrieval varied from ~0.02 to ~0.03, depending on the assumption regarding uncertainty for MFRSR direct-normal irradiance measured at the surface. Obtained Root Mean Square Errors (RMSE ~ 0.025) from the evaluation of MFRSR retrievals against AERONET AOD_{λ} were, in general, lower than estimated MFRSR AOD_{λ} uncertainty, and close to the uncertainty of AERONET field sunphotometers (~ 0.02).

1. Introduction

Aerosol Optical Depth (AOD) is an important variable to characterize atmospheric particles columnar abundance and is also fundamental to estimate their direct radiative forcing in the climate system (Shaw, 1983, Kaufman et al., 2002, Menon, 2004, Satheesh and Srinivasan, 2005). Its relevance is also growing in the context of air quality monitoring from satellite (Hoff and Christopher, 2009, van Donkelaar et al., 2010, van Donkelaar et al., 2013). However, the so called Extraterrestrial Response Calibration (ERC) of the radiometers designed to monitor AOD, for instance sun tracking and shadow-band radiometers (Holben et al., 1998, Harrison and Michalsky, 1994), is a critical issue to the accuracy of AOD retrievals (O'Neill et al., 2005, Sinyuk et al., 2012, di Sarra et al., 2015). Therefore, regular and adequate calibration of sun-tracking and shadow-band radiometers dedicated to monitor AOD is vital (Holben et al., 1998, Eck et al., 1999, Michalsky et al., 2001). The ERC consists in the estimation of the solar energy that would be measured by the instrument at the top of the atmosphere (TOA) or in hypothetical absence of the atmosphere. It remains one of the most critical calibrations to the accuracy of AOD retrieval (Forgan, 1994; Michalsky et al., 2001, Eck et al., 1999; Chen et al., 2013). The classical way to perform ERC is based on the Langley plot method, for which measurements on high mountain tops under clean air and stable conditions are recommended (Shaw et al., 1976, Holben et al., 1998). However, very often, regular trips to very high and clean mountain tops to perform ERC are not possible, either due to the lack of resources or to avoid data collection interruption. Consequently, with the spread of ground based AOD monitoring networks, on site calibration based on multiple Langley plots has been successfully adopted elsewhere (Michalsky et al., 2001, Augustine et al., 2008, Rosario et al., 2008, Mazzola et al., 2010, Michalsky et al., 2013).

During the last decades, Amazonia has been a stage for various intensive and mid to long term atmospheric experiments (Avissar et al., 2002, Silva Dias et al., 2002, Andreae et al., 2004, Martin et al., 2016), performing a large number of field measurements, and regularly including ground-based monitoring of AOD. Given the inherent complex logistics that characterize field experiments in Amazonia, regular trips to distant clean mountain tops, to perform ERC of AOD monitoring devices

operating inside the forest, are a challenge, mainly for long-term sites. Unlike AErosol RObotic NETwork (AERONET) sunphotometers, which have a regular calibration logistic supported by NASA (Holben et al., 1998), other ground-based devices for AOD monitoring operating inside the Amazonia have to find alternative ways to provide regular calibration. Multi-Filter Rotating Shadow-band Radiometers (MFRSR, Harrison and Michalsky, 1994) has been also deployed recurrently in the Amazon basin to monitor spectral and broadband solar irradiance and AOD during specific seasons (Yamasoe and Rosario, 2009, Rosario et al., 2009, Yamasoe et al., 2014, Martin et al., 2016), and more recently focusing in mid and long-term monitoring (Barbosa et al., 2014). An experimental site, located in central Amazonia, and included in the context of the Observations and Modelling of the Green Ocean Amazon (GoAmazon2014/5, Martin et al., 2016) under the reference of T0e, is operating since the year of 2011 a MFRSR as part of a set of instruments to perform long term atmospheric monitoring of convection, radiation, aerosols and cloud properties in Central Amazonia (Barbosa et al., 2014). GoAmazon experimental sites range from time point zero (T0) upwind of pollution associated with Manaus city, Brazil (Figure 1) to sites in the midst (T1) and downwind (T2, T3) of the pollution plume (Martin et al., 2016). The MFRSR is being operated at the T0e site since 2011 without performing its ERC, which prevent its application to retrieve AOD. In this context, the question that drives the focus of the present study is: Does Central Amazonia pristine atmosphere conditions provide successful scenarios for Extraterrestrial Response Calibration? Amazonia atmosphere under pristine conditions have been denominated as Green Ocean due to its very low pollution concentration, comparable to remote ocean areas (Robert et al., 2001, Andreae et al., 2004), which is a fundamental requirement to apply the Langley plot method. To answer the question posed, the present paper describes and discusses methods and results of an effort to calibrate, on site, the cited MFRSR. Its subsequent application to characterize the AOD variability is evaluated against AOD retrievals from a collocated Cimel sunphotometer from AERONET (Holben et al., 1998) also operated at the T0e site. The manuscript is organized as follow: **section 2** describes the experimental site, a brief overview on MFRSR and Langley plot method and AOD retrieval theory, **section 3** consists of results and discussion and final remarks are exposed in **section 4**.

2. Experimental site, instruments, and methods

2.1 Experimental site T0e

The T0e site has been operating continuously since February 2011 in Central Amazonia, up-wind from Manaus city (59º 58' 12''W and 02º 53' 27''S, **Figure 1**), with a set of collocated atmospheric monitoring instruments that include a MFRSR, a Cimel sunphotometer and a Raman lidar (Barbosa et al., 2014). The site main goal is to provide long term characterization of diurnal and seasonal cycles of clouds and convection and the interactions and feedback mechanisms between water vapour, clouds, radiation and aerosol particles. It was incorporated as part of the GoAmazon 2014/15 experiment (Martin et al., 2016) network sites, an international experiment designed to investigate the interactions that involve Amazonia natural atmosphere conditions and the air pollution plume from Manaus city.

Figure 1- T0e site location in Central Amazonia from a zoom in showing the site location upwind of the Manaus City. During the wet season (December to May) the dominant wind direction is from northeast (blue arrow) and during the dry season (June to November) from east (brown arrow). GoAmazon 2014/15 experiment sites relative position to the Manaus city: T2 at downwind, T1 in the midst and T0e upwind of the city (Image source: Google Earth maps).

The GoAmazon2014/5 sites were classified from time point zero (T0) upwind of the plume, to T1 in the midst of the plume, to T2 just downwind of the Manaus, to T3 furthest downwind of Manaus (70 km). Manaus city pollution plume composition includes nitrogen and sulphur oxides, and high concentrations of submicron aerosol particles and soot (Kuhn et al., 2010), which is consistent with the nature of the local major anthropogenic sources of air pollution, vehicle fleet, power plants, and industrial activities. Sá et al. (2017) found that the submicron particles composition is dominated by organic material across the sites upwind and downwind of Manaus, independently of the levels of pollution. However, their study pointed out that, among the sites, the absolute mass concentrations of pollutants vary significantly. Average concentrations downwind of Manaus are 100% to 200% higher than those upwind.

In general, during the wet season, the atmosphere at T0e site is a clean reference, since its location upwind of Manaus prevents the site of being strongly affected by the city pollution plume. Meanwhile, during the dry season the atmospheric column at T0e, likewise large portion of the atmosphere across central Amazonia, is influenced by smoke from biomass burning emissions that occur throughout the Amazon basin.

2.2 Instruments

Multifilter Rotating Shadow-band Radiometer is designed to monitor global-horizontal, diffuse-horizontal and direct-normal solar irradiances at narrow and broadband channels (Harrison et al., 1994). It has been used worldwide to derive columnar aerosol optical properties (Harrison and Michalsky, 1994; Alexandrov et al., 2002; Rosario et al., 2008, Michalsky et al., 2010, Mazzola et al., 2010, Michalsky and LeBaron, 2013), water vapour (Michalsky et al., 1995, Alexandrov et al., 2009, Schneider et al., 2010) and cloud optical properties (Min and Harrison, 1996, Wang and Min, 2008, Kassianov et al., 2011). Direct-normal spectral irradiance ($I_{DN,\lambda}$) at the surface, needed to perform AOD retrievals, is obtained via the difference between global-horizontal and diffuse-horizontal irradiances divided by the cosine of the solar zenith angle (Harrison et al., 1994). Once MFRSR angular and spectral responses are properly

characterized and the automated shadow-band system adequately adjusted, accuracy in $I_{DN,\lambda}$ is expected to be comparable to sunphotometers (Harrison et al., 1994). However, once in field, MFRSR filters transmission may suffer degradation with time (Mychalsky et al., 2001, Michalsky and LeBaron, 2013), which makes regular ERC critically necessary to keep the accuracy of AOD retrievals. The MFRSR of the present study has been operating with sporadic interruptions at T0e providing irradiances measurements at time interval of 1 minute at five narrow-band channels (415, 500, 610, 670 and 870 nm) with half-bandwidth of 10 nm and able to permit AOD retrieval. Given the high cloud cover in central Amazonia, the MFRSR high frequency measurements are crucial to improve the frequency of AOD retrieval under cloudy sky and, therefore, minimizes the AERONET known bias toward clear-sky condition (Levy et al., 2010).

2. 3 Langley plot calibration and uncertainties

Langley plot calibration method is based on Lambert-Beer law (Shaw, 1983), which describes the attenuation of a monochromatic beam propagating through a medium.

$$I_{DN,\lambda} = f(d)\, I_{0,\lambda}\, e^{-m\tau_\lambda} \qquad \text{eq. 1}$$

where, considering the full atmospheric column as a medium, $I_{DN,\lambda}$ is the direct solar spectral irradiance at wavelength λ measured at the surface by the MFRSR, $I_{o,\lambda}$ is the solar spectral irradiance that would be measured in the absence of the atmosphere at Earth-Sun mean distance (d_o), f(d) is a correction factor related to Earth-Sun distance variation (Iqbal, 1983), and m and τ_λ represent the atmosphere relative optical air mass and total optical depth, respectively. Linearization of the equation 1 by applying the natural logarithms to the both sides of the equation leads to a linear relation between m and $\ln(I_{DN,\lambda})$, on which τ_λ and $\ln(f(d)I_{o,\lambda})$ represent, respectively, the angular and linear coefficients.

$$\ln\left(I_{DN,\lambda}\right) = \ln\left(f(d)I_{o,\lambda}\right) - m\tau_\lambda \qquad \text{eq. 2}$$

Knowing $\ln(I_{DN,\lambda})$ over a range of m, during which the atmosphere remained clean and stable, the least-squares regression method can be applied to provide a linear fit formulation between both variables, where the angular coefficient is the mean atmosphere optical depth, and the linear coefficient represents the case of m equal to zero, a hypothetical absence of atmosphere, from which an estimation of the solar extraterrestrial spectral irradiance ($I_{o,\lambda}$) can be made.

In the present study, the atmosphere relative optical air mass (m) was calculated as a function of Solar Zenith Angle (SZA) based on the Kasten and Young (1989) and $\ln(I_{DN,\lambda})$ taken from MFRSR direct-normal irradiance measurements for the years of 2012 and 2015. As we assumed that both, the response variable, $\ln(I_{DN,\lambda})$, and the predictor variable, m, are subject to errors, it was applied the least square regression treatment that consider errors in both adjusted variables (Irvin and Quickenden, 1983). The errors in $\ln(I_{DN,\lambda})$ were obtained through error propagation theory considering Harrison et al. (1994) estimate of uncertainty to MFRSR direct-normal irradiance ($\sigma_{I_{DN,\lambda}} = 2\%$). Regarding error in the airmass (σ_m) we based on the study of Tomasi and Petkov (2014), which compared atmospheric airmass results from Kasten and Young (1989) formulation against rigorous calculation and found differences lower than 0.8%. Therefore, we assumed 0.8% as an estimate of uncertainty to the airmass calculated using Kasten and Young (1989). Following previous studies suggestion (Mazzola et al., 2010 and Alexandrov et al., 2004), to apply least square regression we adopted the airmass range from 2.0 to 5.0. For airmass larger than 5.0, high solar energy incident angles, calibration may be affected by the uncertainty of the MFRSR cosine angle correction and the shadow-band correction, meanwhile low airmasses, near 1.0, increase the probability of turbulent atmospheric conditions and, therefore, the reduction of the optical depth stability (Chen et al., 2013).

The quality of the linear fit derived using least-square regression is highly dependent on optical depth temporal stability, which is more likely to be observed under aerosol background conditions and stable atmosphere. To obtain a set of linear fit able to provide high quality Langley plot calibration samples, for both years 2012 and 2015, were selected only morning cases, to avoid the afternoon vigorous convection, and only linear fit with correlation coefficients (R^2) higher than 0.990. This is the minimal

value usually obtained for calibration performed at high mountain top (Schmid and Wehrli, 1995). Also, considering Schafer et al. (1998) study on AOD climatology across the Amazon basin, only AOD values typical of background conditions were selected. For both years studied, 2012 and 2015, the MFRSR final extraterrestrial spectral response calibration ($< I_{o,\lambda} >$) was estimated from the mean of the correspondent set of extraterrestrial response calibration ($I_{o,\lambda}$) obtained from individual Langley plot calibrations. The uncertainties of the derived final calibrations were estimated as the standard error of the mean ($\sigma_{<I_{o,\lambda}>}$). Subsequently, the final calibrations results were applied to retrieve AOD_λ over the T0e site using the MFRSR.

2.4 Aerosol Optical Depth (AOD_λ) inversion and uncertainty estimate

From equation 2, the atmospheric total optical depth (τ_λ) can be separated as follow:

$$\tau_\lambda = \tau_{m,\lambda} + AOD_\lambda + \tau_{g,\lambda} \qquad eq.3$$

Where $\tau_{m,\lambda}$, $\tau_{g,\lambda}$ represent, respectively, molecular scattering and gas absorption optical depths. All MFRSR channels are affected by molecular scattering, while gas absorption is highly selective, therefore affects specific channels. The most relevant influence of gas absorption on MFRSR channels is produced by ozone (O_3) at 610 and 670 nm channels and by nitrogen dioxide (NO_2) at 415 nm channel. Therefore, combination of the equation 3 and equation 2 leads to the AOD_λ retrieval equation

$$AOD_\lambda = -\frac{1}{m} \ln\left[\frac{I_{DN,\lambda}}{f(d) < I_{o,\lambda} >}\right] - \tau_{m,\lambda} - \frac{m_{O3}}{m}\tau_{O3,\lambda} - \tau_{NO2,\lambda} \qquad eq.4$$

where $\tau_{m,\lambda}$ was calculated using the Kasten and Young (1989) formulation as a function of the climatological surface atmospheric pressure. Given its unique vertical distribution, ozone relative optical air mass (m_{O3}) was estimated separately based on Staehelin et al. (1995). Ozone (O_3) and nitrogen dioxide (NO_2) absorption optical depths over T0e site were obtained considering their spectral cross section absorption and average column content (O_3 = 267.6±5.8 Dobson Units, NO_2=0.076±0.012 Dobson Units) over the years between 2011 and 2015, taken from the SCanning Imaging Absorption

spectroMeter for Atmospheric CHartographY (SCIAMACHY, Bovensmann et al., 1999) and Ozone Monitoring Instrument (OMI, Levelt et al., 2006) products, respectively.

In general, the accuracy of the AOD_λ inversion is dominated by the uncertainty in the extraterrestrial response calibration ($< I_{o,\lambda} >$) and $I_{DN,\lambda}$ measurements (Michalsky et al., 2002, Alexandrov et al., 2007, Mazzola et al., 2010). Typically, uncertainties in both terms are at least one order of magnitude greater than the contributions of the other terms (Mazzola et al., 2010). Considering only the uncertainties in extraterrestrial response calibration ($\sigma_{<I_{o,\lambda}>}$) and in $I_{DN,\lambda}$ measurement ($\sigma_{I_{DN,\lambda}}$), an estimate of uncertainty (σ_{AOD_λ}) of the retrieved AOD_λ can be evaluated as

$$\sigma_{AOD_\lambda} = \sqrt{\left[\frac{1}{m}\frac{\sigma_{<I_{o,\lambda}>}}{< I_{o,\lambda} >}\right]^2 + \left[\frac{1}{m}\frac{\sigma_{I_{DN,\lambda}}}{I_{DN,\lambda}}\right]^2} \qquad \text{eq. 5}$$

where $\sigma_{<I_{o,\lambda}>}$, as described, is based on the standard error of the mean of multiple extraterrestrial responses obtained from a set of individual Langley plot calibration. Evaluation of the uncertainty in $I_{DN,\lambda}$ is a challenge given its dependency on multiple factors, i.e., shadow-band adjustment, accuracy of the angular response and MFRSR positioning regarding misalignment and tilt (Harrison et al., 1994, Alexandrov et al., 2007). Harrison et al. (1994) estimated MFRSR $I_{DN,\lambda}$ typical uncertainty to vary between 2 and 3%. Alexandrov et al. (2007) achieved lower estimation, roughly 1.5% for all channels. Assuming Harrison et al. (1994) maximum uncertainty (3%), the final uncertainty in MFRSR AOD_λ, for all channels, was evaluated for the worst case scenario, i.e., for unit relative air mass($m = 1$).

Additionally, considering AOD_λ at two spectral channels ($\lambda 1, \lambda 2$) as reference, the spectral dependence of AOD_λ was evaluated using Ångström exponent ($\alpha_{\lambda 1,\lambda 2}$), calculated using the following equation

$$\alpha_{\lambda 1,\lambda 2} = -\frac{\ln[AOD_{\lambda 1}/AOD_{\lambda 2}]}{\ln(\lambda 1/\lambda 2)} \qquad \text{eq. 6}$$

Due to its dependency on aerosol particle size distribution (Eck et al., 1999), $\alpha_{\lambda 1,\lambda 2}$ can be used as a qualitative indicator to evaluate the predominance of submicrometric (fine particles) or micrometric

aerosol particles (coarse mode) in the atmosphere. High values of $\alpha_{\lambda1,\lambda2}$, greater than 2.0, indicate dominance of fine aerosol particles, while values lower than 1.0 are typically related to coarse aerosol particles dominance (Eck et al., 1999). In central Amazonia, for regions upwind of Manaus urban area, such as the T0e site, air masses rich in fine aerosol particles are typically associated with smoke transport from biomass burning regions. Air masses dominated by coarse particles fraction are in general associated with local and regional biogenic and soil particles (Artaxo et al., 1998). Eventually, under favourable atmospheric circulation, air mass containing coarse dust particles transported from Sahara Desert may also affect T0e site atmospheric column (Koren et al., 2006, Ben-Ami et al., 2010, Moran-Zuloaga et al.,2018).

Retrievals of AOD_λ and $\alpha_{\lambda1,\lambda2}$ from MFRSR measurements were validated against AERONET direct Sun products Level 2.0 retrieved by a Cimel sunphotometer also installed at T0e site. AERONET provides AOD at seven wavelengths 340, 380, 440, 500, 670, 870 and 1020 nm, being three coincident with MFRSR wavelengths, 500, 670 and 870 nm. In order to evaluate the MFRSR AOD_λ at the remaining channels, 415 and 610 nm, the Ångström Exponent from AERONET was used to perform interpolation to derive AOD_λ in those channels for the network. Specifically, for the comparison purpose, MFRSR AOD_λ at 1 minute rate was averaged within a 5 minute interval centered on AERONET sun-photometer retrieval, large standard deviations from the mean, i.e. higher than 0.08 (considering 4x AERONET field sunphotometer AOD uncertainty, which is 0.02), were interpreted as cloud contamination in MFRSR, therefore excluded from the analysis. Afterwards, MFRSR results were used to describe and analyse the seasonal variability of columnar aerosol particles optical properties over T0e site.

The statistical metrics used to compare MFRSR AOD (AOD_{MFR}) with AERONET sun-photometer AOD (AOD_{Aer}), assuming the later as the reference, are the root mean square error (RMSE), a measure of average deviation from the reference, and Bias, a measure of overall bias error or systematic error:

$$RMSE = \sqrt{\frac{1}{N}\sum_{i=1}^{N}\left(\frac{AOD_{MFR,i} - AOD_{Aer,i}}{AOD_{Aer,i}}\right)^2} \qquad eq.7$$

$$Bias = \frac{1}{N}\sum_{i=1}^{N}\frac{AOD_{MFR,i} - AOD_{Aer,i}}{AOD_{Aer,i}} \quad eq.8$$

3. Results

3.1 MFRSR Langley plot calibration and uncertainty

An example of the diurnal cycle of the spectral solar direct-normal irradiance measured (20 June 2012) by the MFRSR prone to a successful Langley plot is presented in **Figure 2**. In the morning period, before vigorous convection initiates, the direct-normal irradiance at all channels is characterized by a continuous increase. The suitability for a successful Langley plot is evidenced in the quality of the linear fit achieved, as can be confirmed in **Table 1** for the 500 nm channel. **Table 1** and **Table 2** present for the 500 nm channels, respectively, for the years 2012 and 2015, the obtained extraterrestrial response calibrations ($I_{o,\lambda}$) for each individual Langley plot that met the criteria defined, i.e. $R^2 \geq 0.990$ and background AOD. The tables with the results for the remaining channels (415, 610, 670 and 870 nm) are presented in the supplementary material. It is worth to mention that the slopes derived from Langley plot and presented in Tables 1 and 2 represent the daily average of total atmospheric optical depth (including molecular, gaseous absorption and aerosol optical depths). Mean molecular and ozone absorption optical depth in Central Amazonia at the visible spectrum are ~ 0.14 and ~0.01, respectively. Therefore, assuming these typical values, the subtraction of ozone and molecular optical depth from the total atmospheric optical depth (slopes) would result in daily mean AOD values in the range of 0.05 - 0.15, which is typically observed in Amazonia background atmosphere (Schafer et al., 2008).

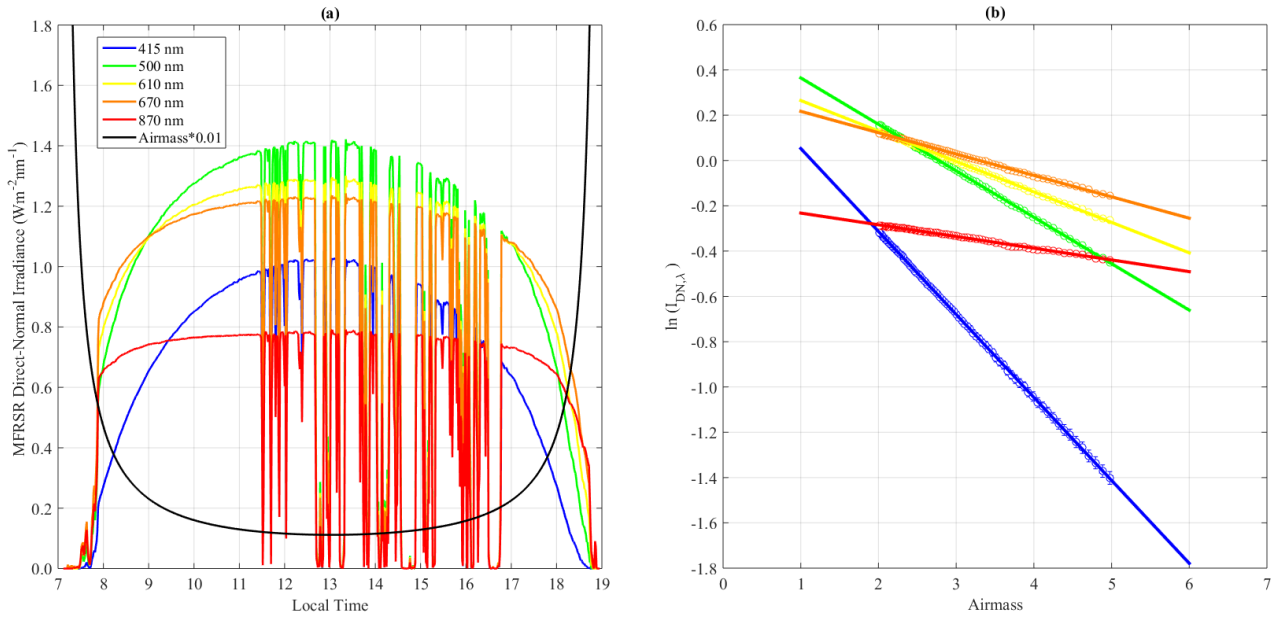

Figure 2 - (a) Diurnal cycle of air mass and direct-normal spectral solar irradiance measured by the MFRSR operating at the T0e site in Central Amazonia. (b) Example of Langley plot calibration applied to MFRSR spectral irradiance measurements taken under the clear sky period (08:00 to 11:00 Local Time) of the diurnal cycle shown in (a). (Day: 20 June 2012)

Table 1 – Individual extraterrestrial calibration results ($I_{o,500nm}$) applying Langley Plot technique to measurements of solar direct-normal irradiance at 500 nm from a MFRSR operating at T0e site in Central Amazônia for the year 2012. The individual uncertainty [**σ_Io.λ**] used to obtain the relative error [**σ_Io.λ (%)**] was estimated from the **intercept** and its respective uncertainty **(σ_intercept**) derived from the least square regression method.

Date	**slope**	**σ_slope**	**intercept**	**σ_intercept**	**$I_{o.500\ nm}$**	**σ_Io.λ (%)**	**R^2**	**N**
17-may-12	-0.2426	0.0016	0.5709	0.0043	1.814	0.434	-0.9992	63
16-jun-12	-0.2450	0.0019	0.6058	0.0055	1.895	0.549	-0.9939	64
17-jun-12	-0.2237	0.0016	0.5560	0.0046	1.803	0.464	-0.9990	61
20-jun-12	-0.2117	0.0015	0.5846	0.0043	1.856	0.434	-0.9992	64
21-jun-12	-0.2261	0.0017	0.5722	0.0047	1.834	0.474	-0.9996	65
22-jun-12	-0.2265	0.0018	0.5362	0.0050	1.769	0.501	-0.9995	71
25-jun-12	-0.2585	0.0019	0.6461	0.0055	1.975	0.546	-0.9992	78
3-jul-12	-0.2493	0.0020	0.5848	0.0058	1.858	0.577	-0.9978	61
4-jul-12	-0.2436	0.0019	0.6060	0.0054	1.898	0.542	-0.9998	63

8-jul-12	-0.2430	0.0020	0.5668	0.0058	1.824	0.581	-0.9996	64
11-jul-12	-0.2420	0.0021	0.5456	0.0059	1.785	0.590	-0.9995	62
1-aug-12	-0.2616	0.0021	0.5843	0.0058	1.848	0.580	-0.9997	64
2-aug-12	-0.2401	0.0020	0.5221	0.0055	1.736	0.549	-0.9920	62
3-aug-12	-0.2775	0.0021	0.6313	0.0058	1.935	0.584	-0.9912	65
4-aug-12	-0.2359	0.0017	0.5751	0.0048	1.829	0.482	-0.9991	62
6-aug-12	-0.2880	0.0025	0.5561	0.0070	1.793	0.700	-0.9987	63
21-dec-12	-0.2658	0.0016	0.6294	0.0042	1.815	0.418	-0.9996	63

Table 2 – Individual extraterrestrial calibration results ($I_{o,500nm}$) applying Langley Plot technique to measurements of solar direct-normal irradiance at 500 nm from a MFRSR operating at T0e site in Central Amazônia for the year 2015. The individual uncertainty [**σ_Io.λ**] used to obtain the relative error [**σ_Io.λ (%)**] was estimated from the **intercept** and its respective uncertainty **(σ_intercept**) derived from the least square regression method.

Date	**slope**	**σ_slope**	**intercept**	**σ_intercept**	**$I_{o.500\ nm}$**	**σ_Io.λ (%)**	**R^2**	**N**
19-feb-15	-0.2045	0.0014	0.5723	0.0041	1.734	0.412	-0.9959	62
27-mar-15	-0.2335	0.0015	0.5957	0.0039	1.809	0.395	-0.9941	69
4-jun-15	-0.2787	0.0021	0.6436	0.0058	1.963	0.583	-0.9923	68
24-jun-15	-0.1900	0.0013	0.5545	0.0039	1.802	0.394	-0.9996	63
1-jul-15	-0.2301	0.0016	0.6247	0.0048	1.933	0.478	-0.9989	62
2-jul-15	-0.2039	0.0015	0.5530	0.0043	1.800	0.433	-0.9995	62
6-jul-15	-0.2397	0.0019	0.6022	0.0054	1.890	0.542	-0.9979	61
10-jul-15	-0.2513	0.0019	0.6256	0.0055	1.934	0.546	-0.9988	61
11-jul-15	-0.2487	0.0019	0.6169	0.0056	1.917	0.556	-0.9996	61
12-jul-15	-0.2634	0.0022	0.5949	0.0063	1.876	0.634	-0.9993	61
15-jul-15	-0.2896	0.0026	0.6070	0.0074	1.898	0.745	-0.9994	61
28-jul-15	-0.2606	0.0020	0.6344	0.0056	1.945	0.555	-0.9982	62
29-jul-15	-0.2496	0.0021	0.5611	0.0059	1.807	0.585	-0.9901	62
30-jul-15	-0.2406	0.0018	0.5912	0.0051	1.862	0.510	-0.9964	62
1-aug-15	-0.2500	0.0019	0.6162	0.0054	1.908	0.536	-0.9954	62
2-aug-15	-0.2907	0.0024	0.6385	0.0066	1.950	0.657	-0.9983	62

7-aug-15	-0.2535	0.0018	0.6151	0.0051	1.902	0.508	-0.9997	64
23-aug-15	-0.2652	0.0018	0.6047	0.0048	1.870	0.482	-0.9987	69
5-sep-15	-0.2623	0.0018	0.5373	0.0044	1.737	0.438	-0.9983	74
9-sep-15	-0.2411	0.0014	0.6266	0.0038	1.895	0.376	-0.9996	75
22-sep-15	-0.2825	0.0018	0.5998	0.0045	1.831	0.454	-0.9992	75

The final extraterrestrial response estimations $< I_{o,\lambda} >$, for both years and all channels, based on average of all individual Langley plot calibration, are presented in **Table 3** along with the standard error from the mean as the uncertainty $(\sigma_{<I_{o,\lambda}>})$, sample number (N) and the relative difference between calibration estimated for 2012 and 2015. The relative uncertainties among the channels varied from 0.7% (870 nm) to 1.0% (415 nm) in 2012, and from 0.4% (870 nm) to 1.0% (415 nm) in 2015, which are surprisingly satisfactory for conditions diverse from those recommended (clean top mountain). Regarding the relative difference (-0.4%) between calibration constant derived for the two years, the difference for the channel 415 nm is not statistically significant, suggesting that between 2012 and 2015 the correspondent transmission filter did not suffer relevant degradation. Meanwhile, a drift of 4.8 % was observed for the 870 nm channel, an indication of the lower stability of its transmission filter. The remaining channels (500, 613, 670 nm) calibrations constant, opposite to the 870 nm channel, presented positive trend between 2012 and 2015 calibrations. However, given the values of the uncertainty $(\sigma_{<I_{o,\lambda}>})$ in their calibration constants, we are not able to attest that 500, 613 and 670 nm channels have statistically suffered degradation.

Table 3 – MFRSR final extraterrestrial calibrations estimates $< I_{o,\lambda} >$ for the years 2012 and 2015 averaging results of individual Langley plot calibration from Table 1, Table 2 and tables in the supplementary material. The uncertainty estimation $(\sigma_{<I_{o,\lambda}>})$ is based on the correspondent standard error of the average.

	Year 2012			**Year 2015**			**Difference (%)**
Channels	**N**	$\mathbf{<I_{o\lambda}>}$	$\boldsymbol{\sigma_{<I_{o,\lambda}>}}$	**N**	$\mathbf{<I_{o\lambda}>}$	$\boldsymbol{\sigma_{<I_{o,\lambda}>}}$	$\boldsymbol{\Delta<I_{o,\lambda}>}$ **(2012-2015)**
415 nm	21	1.586	0.015 (1.0 %)	22	1.579	0.017 (1.0%)	-0.4

500 nm	17	1.839	0.015 (0.8 %)	21	1.870	0.015 (0.8%)	+1.7
613 nm	14	1.545	0.010 (0.7%)	17	1.572	0.011 (0.7%)	+1.8
670 nm	15	1.416	0.010 (0.7%)	18	1.433	0.008 (0.6%)	+1.2
870 nm	15	0,842	0.008 (0.9%)	20	0.802	0.003 (0.4%)	-4.8

Considering the estimate uncertainties in the extraterrestrial calibration constant (0.4% -1.0%), and the Harrison et al. (1994) maximum uncertainty (3%) for MFRSR $I_{DN,\lambda}$ measurements, accordingly to the error propagation analysis (equation 6), the worst estimative (i.e., for unit airmass) for our absolute uncertainty in AOD_{λ} is ~ 0.03, which is comparable with uncertainty of AOD_{λ} retrieved from AERONET field sunphotometers measurements (~0.02, Eck et al., 1999). However, if a lower uncertainty in $I_{DN,\lambda}$ is assumed, for instance 1.5% (as suggested by Alexandrov et al., 2007), that would reduce MFRSR AOD_{λ} uncertainty from ~0.03 to ~ 0.02.

In general, perfect linear Langley plots are associated with stable AOD, however it is possible that not all nearly linear Langley plots are able to provide correct calibration. Airmass assumption, mainly regarding aerosol particles airmass (Schmid and Wehrli, 1995), instruments induced artefact, the shadow-band system alignment (Chen et al., 2013), may contribute to error in calibration. These influences are all challenge to estimate. Therefore, taking the mean of a set of individual Langley plot calibration as the best estimate for the final calibration constant, along with the comparison of the AOD results with AERONET sunphotometer retrievals should provide a good reference to evaluate the quality of the calibration constant obtained. The results obtained for RMSEs derived from the comparison between MFRSR retrievals and AERONET sunphotometer AOD are lower than the estimated uncertainty for MFRSR AOD_{λ} retrievals (i.e., ~0.02 - 0.03, depending on the $I_{DN,\lambda}$ uncertainty assumed, 1.5 or 3 %) and just above the maximum uncertainty for AERONET field instrument (~0.02), demonstrating that, in spite of eventual error associated with assumption made during the Langley plot application, the final derived constants are able to provide reliable AOD retrievals.

3.2 Aerosol Optical Depth (AOD_λ) inversion and uncertainty estimate

Once determined the MFRSR channels final extraterrestrial response calibration, direct-normal irradiance measurements taken along 2012 and 2015 were applied to retrieve AOD_λ and to calculate Ångström Exponent. **Figure 3** illustrates, for a specific day (22 November 2012), results of cloud screening and a comparison between the diurnal variability of AOD_λ from MFRSR and AERONET sunphotometer. The cloud screening criteria captured the majority of contaminated measurements, but few suspicious remaining points are likely related to optically thin cirrus. A more conservative algorithm would remove a significant amount of cloud free cases, as seems to be the case for AERONET sunphotometer retrievals. The intercomparison showed the consistency of MFRSR retrievals regarding AOD_λ diurnal variability. It is worth to emphasize the higher frequency of MFRSR retrieval during the afternoon when compared with AERONET product. This is a critical aspect regarding the representativity of AOD_λ diurnal variation in regions marked by strong diurnal cycle of convection and cloud cover such as Central Amazonia. The MFRSR 1-min frequency is expected to improve the statistic of AOD under cloudy conditions, since AERONET sunphotometer current statistics are recognized to be biased toward cloudless sky conditions (Levy et al., 2010).

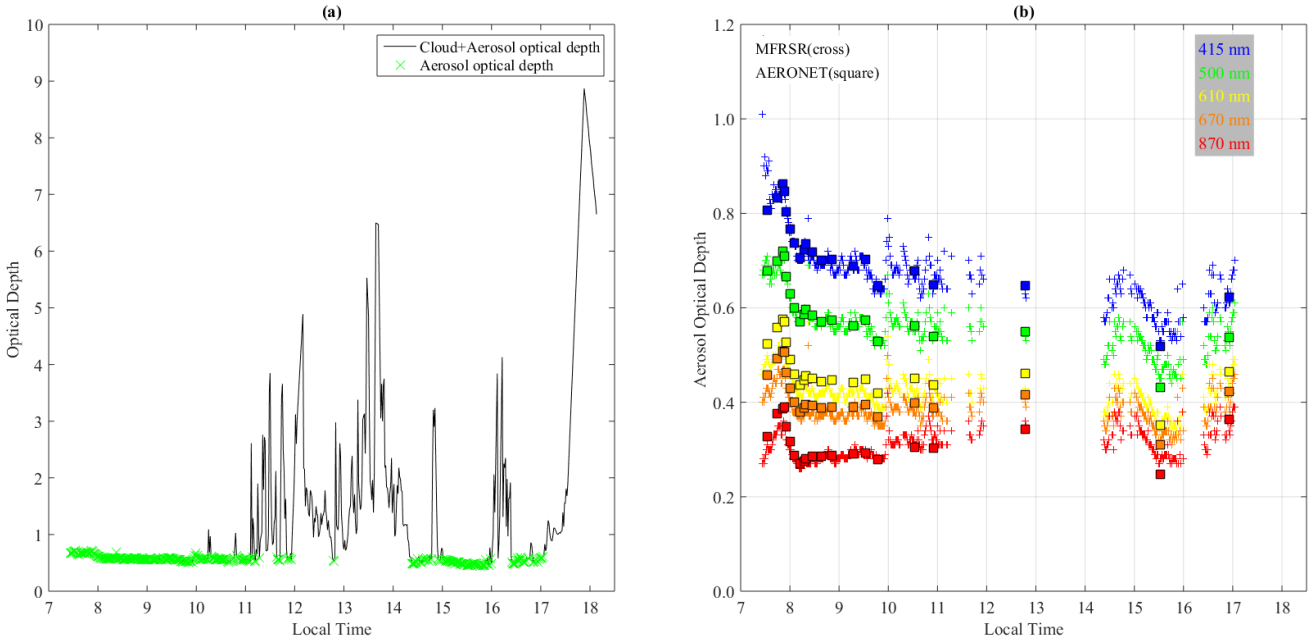

Figure 3 - (a) Example of the cloud screening applied to the MFRSR aerosol optical depth retrievals (22 November 2012). (b) Cloud screened diurnal cycle of multichannel aerosol optical depth from MFRSR compared with AOD retrievals from AERONET Level 2.0 product.

A comparison focusing on seasonal variability was also performed. **Figure 4** presents the 2012 seasonal variability of $AOD_{500\,nm}$ and $\alpha_{415,670\,nm}$ over T0e site as seen by MFRSR (based on 1 min time resolution) and AERONET sunphotometer. When all MFRSR instantaneous retrievals are analysed against AERONET sunphotometer AOD there is an apparent overestimation of AOD and underestimation of Ångström Exponent (AE). However, when analysing only coincident retrievals in time of both MFRSR and AERONET sunphotometer, the AOD and most of AE results are consistent. Therefore, the apparent higher AOD retrievals and low AE seen in MFRSR results are related to period during which AERONET AOD product does not provide retrieval. MFRSR retrievals were able to represent consistently the major seasonal features. From March to June, central Amazonia presents its lowest $AOD_{500\,nm}$ levels, ranging from ~0.05 to ~0.20. In a completely opposite scenario, during the biomass burning season (August to November), $AOD_{500\,nm}$ hardly goes down below 0.20 and values above 0.50 are quite frequent. During the transition periods, from background conditions to biomass burning (June to July) and from biomass burning to background (December to February), $AOD_{500\,nm}$ values oscillated between typical background

and biomass burning season. Considering that the enhancement of AOD_{λ} during the biomass burning season across central Amazonia is dominated by increase in small particles (Eck et al., 1999, Rosario, 2011), $\alpha_{415,670\,nm}$ variability (**Figure 4**) is consistent with the AOD_{500} discussion, i. e., as the aerosol loading increases from July to the biomass burning months (Aug-Sep-Oct-Nov), $\alpha_{415,670\,nm}$ also shows an enhancement. Ångström Exponents ranging from 0.4 to 0.8, which are dominant under background conditions, became rare throughout the biomass burning season and intermittent during the transition periods, a feature consistently described by MFRSR and AERONET sunphotometer. Similar results, for both AOD_{500} and $\alpha_{415,670\,nm}$ were observed regarding the year 2015 (not shown here).

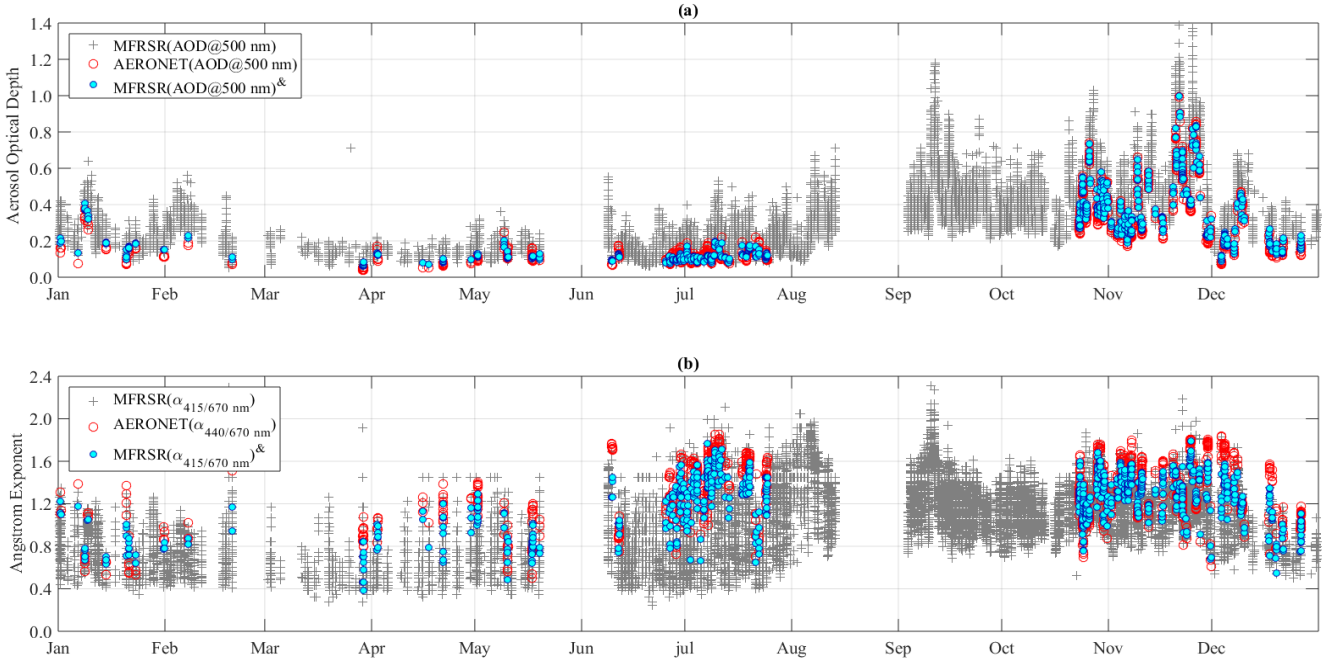

Figure 4 –Seasonal variability of (a) Aerosol Optical Depth and (b) Ångström exponent (AE) at the visible spectrum region in Central Amazonia for the year 2012. MFRSR (AOD@500 nm) represents MFRSR instantaneous AOD retrieval at 1 min rate; MFRSR (AOD@500 nm)$^{\&}$ represents only MFRSR AOD retrieved colocated in time with AERONET sunphotometer AOD retrieval (AERONET (AOD@500 nm)). MFRSR ($\alpha_{415,670\,nm}$) represents MFRSR instantaneous AE at 1 min rate; MFRSR ($\alpha_{415,670\,nm}$)$^{\&}$ represents only MFRSR AE retrieved colocated in time with AERONET sunphotometer AE retrieval (AERONET ($\alpha_{440,670\,nm}$)).

Figures 5 and **6** show scatter plots and statistic metrics (Bias, RMSE and correlation coefficient) comparing MFRSR and AERONET sunphotometer retrievals for 2012 and 2015, respectively. In general,

there is a good agreement between both AOD_λ retrievals. However, non-negligible trends are seen, especially for 2012, and in particular for the lower and higher AOD edges. For low AOD_λ values, a systematic underestimation by MFRSR is observed for all channels, while for high AOD_λ , the longer wavelength channels (610 and 670 nm) tend to underestimate AOD. The year 2015 trends are less evident, mainly for the low aerosol loading when compared with 2012. Nevertheless, overall, the statistics metrics used to evaluate MFRSR retrievals performance against AERONET sunphotometer suggest that, when is not possible to perform high top mountain calibration, the extraterrestrial response calibration performed at Central Amazonia has reliability to support consistent retrievals of AOD. The obtained RMSEs are lower than the estimated uncertainty for MFRSR AOD_λ retrievals (i.e., ~0.02 - 0.03, depending on the $I_{DN,\lambda}$ uncertainty assumed) and slightly above the maximum uncertainty for AERONET field instrument (~0.02).

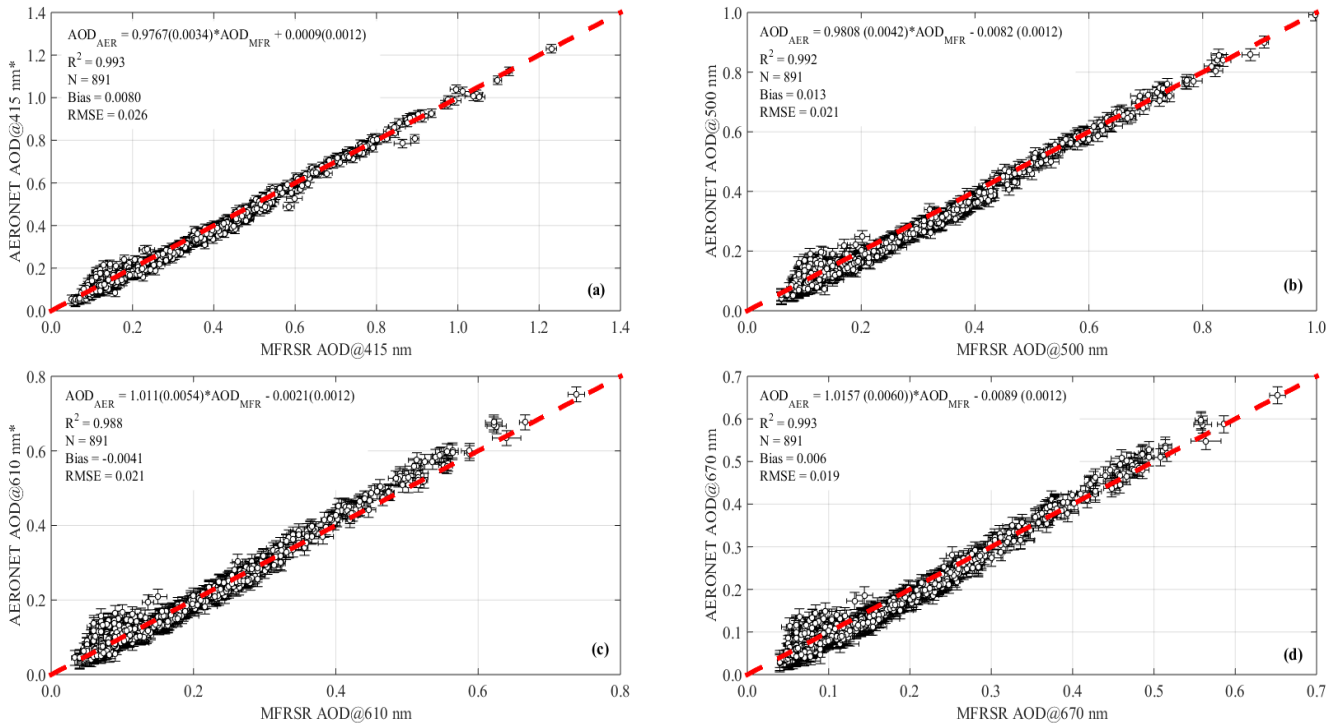

Figure 5 - Spectral AOD retrieval from the on-site calibrated MFRSR as a function of AOD from AERONET direct Sun product level 2.0 for the year 2012. The asterisk (*) indicates that the AOD at that wavelength was estimated using Ångström Exponent and the red dashed line represents the 1:1 line.

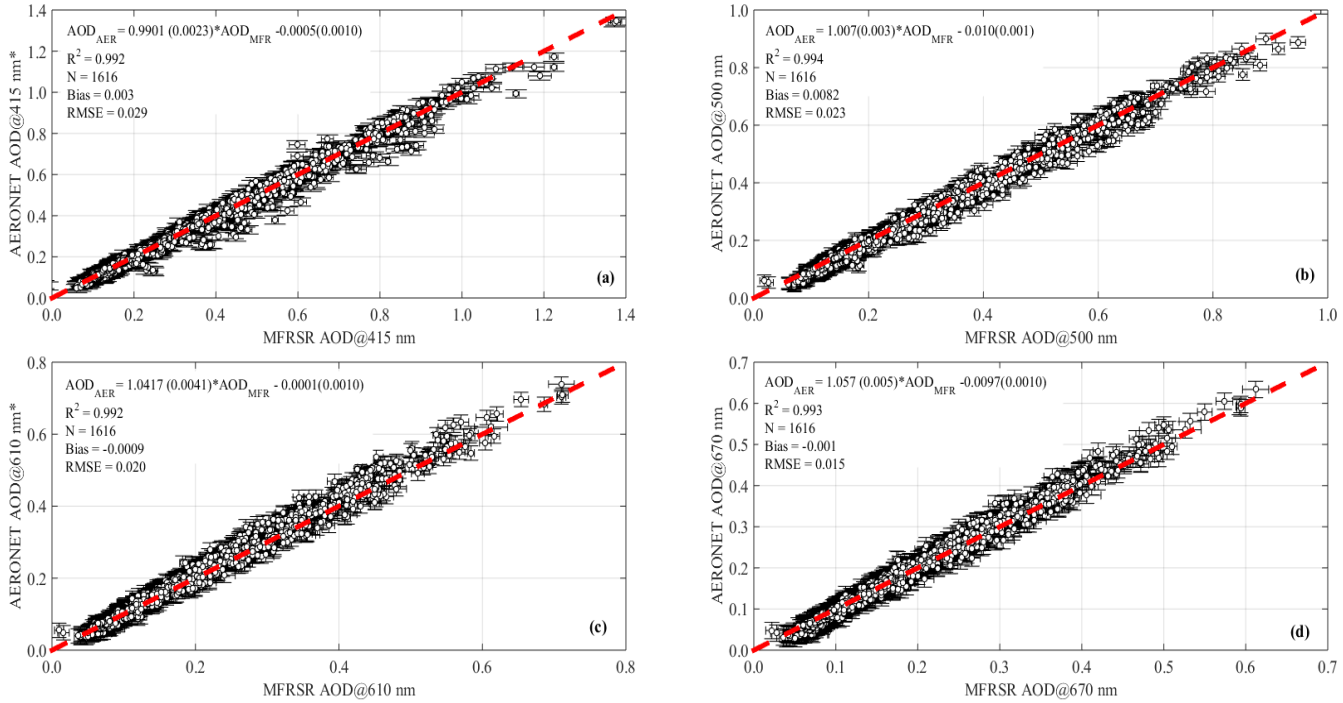

Figure 6 - Spectral AOD retrieval from the on-site calibrated MFRSR as a function of AOD from AERONET direct Sun product level 2.0 for the year 2015. The asterisk (*) indicates that the AOD at that wavelength was estimated using Ångström exponent and the red dashed line represents 1:1 line.

Figure 7 compares Ångström Exponents derived using AOD retrieved from AERONET sunphotometer and MFRSR measurements, although comparisons are not as good as that observed for AOD, MFRSR results provides consistent range of Ångström Exponent in respect to the AERONET results.

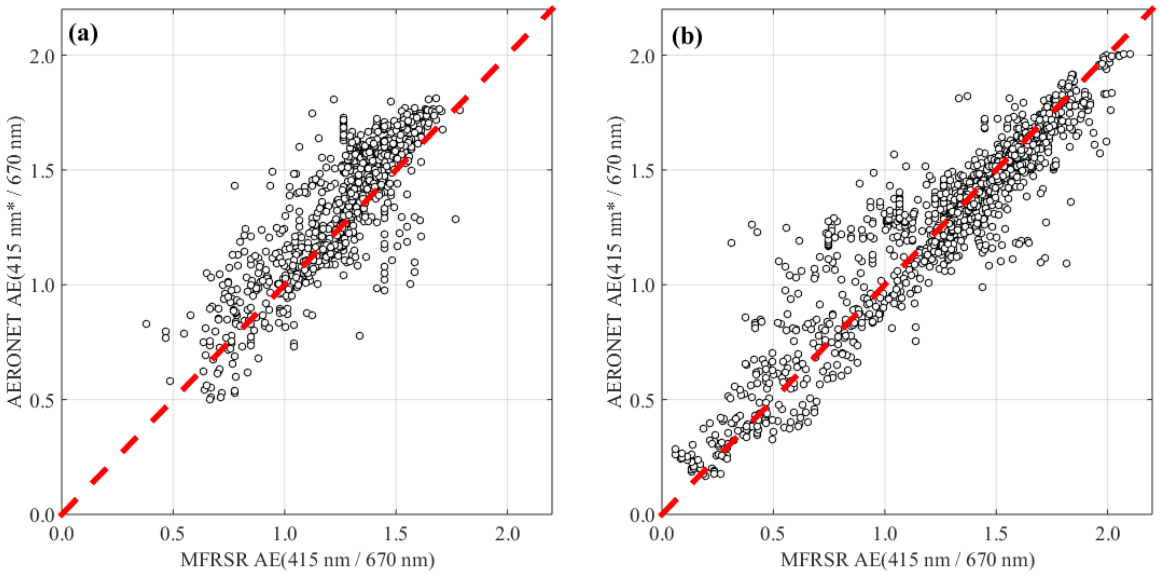

Figure 7 – Ångström Exponent (AE) for visible spectrum derived using AOD at 415 nm and 670 nm from the on-site calibrated MFRSR as a function of AE derived from AOD at 415 nm* and 670 nm corresponding to the AERONET direct Sun product level 2.0 for the years (a) 2012 and (b) 2015. The

asterisk (*) indicates that AERONET AOD at 415 nm was estimated using AE since this channel is not present in network sunphotometers. The red dashed line represents 1:1 line.

4. Conclusions

Does Central Amazonian pristine atmosphere provide successful extraterrestrial response calibration based on Langley plot method? This question emerged from the challenge to maintain regular calibration of a MFRSR dedicated to long-term retrieval of columnar aerosol optical properties in central Amazon. To answer the question, the MFRSR was calibrated on site using the Langley plot method for two distinct years, 2012 and 2015, and subsequently applied to retrieve aerosol columnar optical properties, i.e., AOD and Ångström Exponent (AE). Retrievals were evaluated against direct sun inversion products (Level 2.0) from a collocated Cimel sunphotometer belonging to AERONET. Results obtained show that on site calibration using Langley plot, under Amazonian pristine conditions, is able to provide extraterrestrial response with relative uncertainties varying from ~0.4 to ~1.0 % at MFRSR visible channels. The worst estimative (airmass = 1) for absolute uncertainty in retrieved AOD_{λ} can vary from ~0.03 to ~0.02, depending on the assumption regarding the uncertainty assumed for MFRSR direct-normal irradiance measured at the surface $\left(I_{DN,\lambda} \right)$, which in the literature varies from 1.5% to 3.0%. All Root Mean Square Error (RMSE), obtained from the comparison of MFRSR retrievals against AERONET sunphotomer AOD_{λ} for coincident channels (500 and 670 nm), were lower (< 0.025) than the estimated MFRSR AOD_{λ} uncertainties and close to AERONET field sunphotometers (~ 0.02). Under the point of view of the question posed, these results suggest that on site calibration in central Amazonia pristine conditions is able to provide consistent retrieval of AOD_{λ}. Another relevant aspect of the results provided by the MFRSR, due to its high measurement frequency (one minute), is the improvement of the statistics of AOD under cloudy conditions, which is critical for Amazonia. AERONET sunphotometer current statistics are expected to be biased to cloudless sky conditions, which are dominant during the morning period and dry season.

Competing interests. The authors declare that there are no competing interests.

Acknowledgements. The authors would like to EMBRAPA, INPA, and the LBA Central office for logistical support. Special thanks to Marcelo Rossi, Victor Souza, and Jocivaldo Souza at EMBRAPA, and to Ruth Araujo, Roberta Souza, Bruno Takeshi, and Glauber Cirino from LBA. Henrique Barbosa acknowledges the financial support from FAPESP Research Program on Global Climate Change under research grants 2008/58100-1, 2012/16100-1, 2013/50510-5, and 2013/05014-0. Theotonio Pauliquevis acknowledges the financial support from CNPq research grant 458017/2013-2. Boris Barja acknowledges the financial support of CAPES project A016_2013 on the program Science without Frontiers and the SAVERNET project.

References

Alexandrov, M. D., Lacis, A. A., Carlson, B. E., and Cairns, B.: Remote Sensing of Atmospheric Aerosols and Trace Gases by Means of Multifilter Rotating Shadowband Radiometer. Part II: Climatological Applications, Journal of the Atmospheric Sciences, 59, 544–566, https://doi.org/10.1175/1520-0469(2002)059<0544:RSOAAA>2.0.CO;2, 2002.

Alexandrov, M. D., Kiedron, P., 5 Michalsky, J. J., Hodges, G., Flynn, C. J., and Lacis, A. A.: Optical depth measurements by shadow-band radiometers and their uncertainties, Appl. Opt., 46, 8027–8038, https://doi.org/10.1364/AO.46.008027, 2007.

Andreae, M. O., Rosenfeld, D., Artaxo, P., Costa, A. A., Frank, G. P., Longo, K. M., and Silva-Dias, M. A. F.: Smoking Rain Clouds over the Amazon, Science, 303, 1337–1342, https://doi.org/10.1126/science.1092779, 2004.

Artaxo, P., Fernandas, E. T., Martins, J. V., Yamasoe, M. A., Hobbs, P. V., Maenhaut, W., Longo, K. M., and Castanho, A.: 10 Large-scale aerosol source apportionment in Amazonia, Journal of Geophysical Research: Atmospheres, 103, 31 837–31 847, https://doi.org/10.1029/98JD02346, 1998.

Augustine, J. A., Hodges, G. B., Dutton, E. G., Michalsky, J. J., and Cornwall, C. R.: An aerosol optical depth climatology for NOAA's national surface radiation budget network (SURFRAD), Journal of Geophysical Research: Atmospheres, 113, n/a–n/a, https://doi.org/10.1029/2007JD009504, d11204, 2008.

Avissar, R., Silva Dias, P. L., Silva Dias, M. A. F., and Nobre, C.: The Large-Scale Biosphere-Atmosphere Experiment in Amazonia(LBA): Insights and future research needs, Journal of Geophysical Research: Atmospheres, 107, LBA 54–1–LBA 54–6, https://doi.org/10.1029/2002JD002704, 8086, 2002.

Barbosa, H. M. J., Barja, B., Pauliquevis, T., Gouveia, D. A., Artaxo, P., Cirino, G. G., Santos, R. M. N., and Oliveira, A. B.: A permanente Raman lidar station in the Amazon: description, characterization, and first results, Atmospheric Measurement Techniques, 7, 1745–1762, 20 https://doi.org/10.5194/amt-7-1745-2014, 2014.

Ben-Ami, Y., Koren, I., Rudich, Y., Artaxo, P., Martin, S. T., and Andreae, M. O.: Transport of North African dust from the Bodélé depression to the Amazon Basin: a case study, Atmospheric Chemistry and Physics, 10, 7533–7544, https://doi.org/10.5194/acp-10-7533-2010, 2010.

Bovensmann, H., Burrows, J. P., Buchwitz, M., Frerick, J., Noël, S., Rozanov, V. V., Chance, K. V., and Goede, A. P. H.: SCIAMACHY: Mission Objectives and Measurement Modes, Journal of the Atmospheric Sciences, 56, 127–150, https://doi.org/10.1175/1520- 25 0469(1999)056<0127:SMOAMM>2.0.CO;2, 1999.

Chen, M., Davis, J., Tang, H., Ownby, C., and Gao,W.: The calibration methods for Multi-Filter Rotating Shadowband Radiometer: a review, Frontiers of Earth Science, 7, 257–270, https://doi.org/10.1007/s11707-013-0368-9, 2013.

di Sarra, A., Sferlazzo, D., Meloni, D., Anello, F., Bommarito, C., Corradini, S., Silvestri, L. D., Iorio, T. D., Monteleone, F., Pace, G.,Piacentino, S., and Pugnaghi, S.: Empirical correction of multifilter rotating shadowband radiometer (MFRSR) aerosol optical depths for the aerosol forward scattering and development of a long-term integrated MFRSR-Cimel dataset at Lampedusa, Appl. Opt., 54, 2725– 2737, https://doi.org/10.1364/AO.54.002725, 2015.

Eck, T. F., Holben, B. N., Reid, J. S., Dubovik, O., Smirnov, A., O'Neill, N. T., Slutsker, I., and Kinne, S.: Wavelength dependence of the optical depth of biomass burning, urban, and desert dust aerosols, Journal of Geophysical Research: Atmospheres, 104, 31 333–31 349, https://doi.org/10.1029/1999JD900923, 1999.

Forgan, B. W.: General method for calibrating Sun photometers, Appl. Opt., 33, 4841–4850, https://doi.org/10.1364/AO.33.004841, 1994.

Gueymard, C. A.: Interdisciplinary applications of a versatile spectral solar irradiance model: A review, Energy, 30, 1551 – 1576, https://doi.org/https://doi.org/10.1016/j.energy.2004.04.032, measurement and Modelling of Solar Radiation and Daylight- Challenges for the 21st Century, 2005.

Harrison, L. and Michalsky, J.: Objective algorithms for the retrieval of optical depths from ground-based measurements, Appl. Opt., 33, 5 5126–5132, https://doi.org/10.1364/AO.33.005126, 1994.

Harrison, L., Michalsky, J., and Berndt, J.: Automated multifilter rotating shadow-band radiometer: an instrument for optical depth and radiation measurements, Appl. Opt., 33, 5118–5125, https://doi.org/10.1364/AO.33.005118, 1994.

Hoff, R. M. and Christopher, S. A.: Remote Sensing of Particulate Pollution from Space: Have We Reached the Promised Land?, Journal of the Air & Waste Management Association, 59, 645–675, https://doi.org/10.3155/1047-3289.59.6.645, 2009.

10 Holben, B., Eck, T., Slutsker, I., Tanré, D., Buis, J., Setzer, A., Vermote, E., Reagan, J., Kaufman, Y., Nakajima, T., Lavenu, F., Jankowiak, I., and Smirnov, A.: AERONET—A Federated Instrument Network and Data Archive for Aerosol Characterization, Remote Sensing of Environment, 66, 1 – 16, https://doi.org/https://doi.org/10.1016/S0034-4257(98)00031-5, 1998.

Iqbal, M.: An Introduction to Solar Radiation, Academic Press, San Diego, California, 1983.

Irvin, J. A. and Quickenden. Terry I. Linear least squares treatment when there are errors in both x and y. Journal of Chemical Education 1983 60 (9), 711 DOI: 10.1021/ed060p711

Kassianov, E., Barnard, J., Berg, L. K., Long, C. N., and Flynn, C.: Shortwave spectral radiative forcing of cumulus clouds from surface observations, Geophysical Research Letters, 38, n/a–n/a, https://doi.org/10.1029/2010GL046282, l07801, 2011.

Kasten, F. and Young, A. T.: Revised optical air mass tables and approximation formula, Appl. Opt., 28, 4735–4738,

https://doi.org/10.1364/AO.28.004735, 1989.

Kaufman, Y. J., Tanre, D., and Boucher, O.: A satellite view of aerosols in the climate system, Nature, 419, 215–223, 2002.

Koren, I., Kaufman, Y. J., Washington, R., Todd, M. C., Rudich, Y., Martins, J. V., and Rosenfeld, D.: The Bodélé depression: a single spot in the Sahara that provides most of the mineral dust to the Amazon forest, Environmental Research Letters, 1, 014 005, 2006.

Kuhn, U., Ganzeveld, L., Thielmann, A., Dindorf, T., Schebeske, G., Welling, M., Sciare, J., Roberts, G., Meixner, F. X., Kesselmeier, J., Lelieveld, J., Kolle, O., Ciccioli, P., Lloyd, J.,Trentmann, J., Artaxo, P., and Andreae, M. O.: Impact of ManausCity on the Amazon Green Ocean atmosphere: ozone production, precursor sensitivity and aerosol load, Atmos. Chem. Phys., 10, 9251–9282, doi:10.5194/acp-10-9251-2010, 2010

Levelt, P. F., van den Oord, G. H. J., Dobber, M. R., Malkki, A., Visser, H., de Vries, J., Stammes, P., Lundell, J. O. V.,

and Saari, H.: The ozone monitoring instrument, IEEE Transactions on Geoscience and Remote Sensing, 44, 1093–1101, https://doi.org/10.1109/TGRS.2006.872333, 2006.

Levy, R. C., Remer, L. A., Kleidman, R. G., Mattoo, S., Ichoku, C., Kahn, R., and Eck, T. F.: Global evaluation of the Collection 5 MODIS dark-target aerosol products over land, Atmospheric Chemistry and Physics, 10, 10 399–10 420, https://doi.org/10.5194/acp-10-10399-2010, 2010.

Martin, S. T., Artaxo, P., Machado, L. A. T., Manzi, A. O., Souza, R. A. F., Schumacher, C.,Wang, J., Andreae, M. O., Barbosa, H. M. J., Fan, J., Fisch, G., Goldstein, A. H., Guenther, A., Jimenez, J. L., Pöschl, U., SilvaÂ Dias, M. A., Smith, J. N., and Wendisch, M.: Introduction: Observations and Modeling of the Green Ocean Amazon (GoAmazon2014/5), Atmospheric Chemistry and Physics, 16, 4785–4797, https://doi.org/10.5194/acp-16-4785-2016, 2016.

Mazzola, M., Lanconelli, C., Lupi, A., Busetto, M., Vitale, V., and Tomasi, C.: Columnar aerosol optical properties in the Po Valley, Italy, from MFRSR data, Journal of Geophysical Research: Atmospheres, 115, n/a–n/a, https://doi.org/10.1029/2009JD013310, d17206, 2010.

Menon, S.: Current Uncertainties In Assessing Aerosol Effects On Climate, Annual Review of Environment and Resources, 29, 1–30, https://doi.org/10.1146/annurev.energy.29.063003.132549, 2004.

Michalsky, J. and LeBaron, B.: Fifteen-year aerosol optical depth climatology for Salt Lake City, Journal of Geophysical Research: Atmospheres, 118, 3271–3277, https://doi.org/10.1002/jgrd.50329, 2013.

Michalsky, J., Denn, F., Flynn, C., Hodges, G., Kiedron, P., Koontz, A., Schlemmer, J., and Schwartz, S. E.: Climatology

of aerosol optical depth in north-central Oklahoma: 1992–2008, Journal of Geophysical Research: Atmospheres, 115,

https://doi.org/10.1029/2009JD012197, d07203, 2010.

Michalsky, J. J., Liljegren, J. C., and Harrison, L. C.: A comparison of Sun photometer derivations of total column water vapor and ozone to standard measures of same at the Southern Great Plains Atmospheric Radiation Measurement site, Journal of Geophysical Research: Atmospheres, 100, 25 995–26 003, https://doi.org/10.1029/95JD02706, 1995.

Michalsky, J. J., Schlemmer, J. A., Berkheiser, W. E., Berndt, J. L., Harrison, L. C., Laulainen, N. S., Larson, N. R., and Barnard, J. C.: Multiyear measurements of aerosol optical depth in the Atmospheric Radiation Measurement and Quantitative Links programs, Journal of Geophysical Research: Atmospheres, 106, 12 099–12 107, https://doi.org/10.1029/2001JD900096, 2001.

Min, Q. and Harrison, L. C.: Cloud properties derived from surface MFRSR measurements and comparison with GOES results at the ARM SGP Site, Geophysical Research Letters, 23, 1641–1644, https://doi.org/10.1029/96GL01488, 1996.

Moran-Zuloaga, D., Ditas, F., Walter, D., Saturno, J., Brito, J., Carbone, S., Chi, X., Hrabe de Angelis, I., Baars, H., Godoi, R. H. M., Heese, B., Holanda, B. A., Lavri ˇ c, J. ˇ V., Martin, S. T., Ming, J., Pöhlker, M. L., Ruckteschler, N., Su, H., Wang, Y., Wang, Q., Wang, Z., Weber, B., Wolff, S., Artaxo, P., Pöschl, U., Andreae, M. O., and Pöhlker, C.: Long-term study on coarse mode aerosols in the Amazon rain forest with the frequent intrusion of Saharan dust plumes, Atmos. Chem. Phys., 18, 10055-10088, https://doi.org/10.5194/acp-18-10055-2018, 2018

O'Neill, N. T., McArthur, L. J. B., and Strawbridge, K. B.: Recent progress in the remote sensing of aerosols, Physics in Canada, Special issue on Planetary Remote Sensing in Canada, 61, 235–241, 2005.

Roberts, G. C., Andreae, M. O., Zhou, J., and Artaxo, P.: Cloud condensation nuclei in the Amazon Basin: "marine" conditions over a continent?, Geophysical Research Letters, 28, 2807–2810, https://doi.org/10.1029/2000GL012585, 2001.

Rosario, N.: Variability of aerosol optical properties over South America and the impacts of direct radiative effect of aerosols from biomass burning, Ph.D. thesis, Institute of Astronomy, Geophysics and Atmospheric Sciences, University of São Paulo, 2011.

Rosario, N., Yamasoe, M. A., Sayao, A., and Siqueira, R.: Multifilter rotating shadowband radiometer calibration for spectral aerosol optical depth retrievals over Sao Paulo City, Brazil, Appl. Opt., 47, 1171–1176, https://doi.org/10.1364/AO.47.001171, 2008.

Rosario, N. E., Yamasoe, M. A., and Longo, K. M.: Aerosol Optical Depth and Ångström Coefficient retrievals over the Amazon Forest during 2007 biomass burning season, AIP Conference Proceedings, 1100, 494–497, https://doi.org/10.1063/1.3117029, 2009.

Sá, Suzane S., Brett B. Palm, Pedro Campuzano-Jost, Douglas A. Day, Weiwei Hu, Gabriel Isaacman-VanWertz, Lindsay D. Yee, Joel Brito, Samara Carbone, Igor O. Ribeiro, Glauber G. Cirino, Yingjun Liu, Ryan Thalman, Arthur Sedlacek, Aaron Funk, Courtney Schumacher, John E. Shilling, Johannes Schneider, Paulo Artaxo, Allen H. Goldstein, Rodrigo A. F. Souza, Jian Wang, Karena A. McKinney, Henrique Barbosa, M. Lizabeth Alexander, Jose L. Jimenez, and Scot T. Martin. Atmos. Chem. Phys., 18, 12185-12206, https://doi.org/10.5194/acp-18-12185-2018, 2018

Satheesh, S. K. and Srinivasan, J.: A method to infer short wave absorption due to aerosols using satellite remote sensing, Geophysical Research Letters, 32, https://doi.org/10.1029/2005GL023064, l13814, 2005.

Schafer, J. S.; T. F. Eck; B. N. Holben; P. Artaxo; A. F. Duarte, 2008: Characterization of the optical properties of atmospheric aerosols in Amazonia from long-term AERONET monitoring (1993-1995 and 1999-2006). Journal of Geophysical Research: Atmospheres, 113, D04204, https://doi.org/10.1029/2007JD009319

Schmid, B., and C. Wehrli, Comparison of the sun photometer calibration by use of the Langley technique and the standard lamp, Appl. Opt., 34, 4500–4512, 1995.

Schneider, M., Romero, P. M., Hase, F., Blumenstock, T., Cuevas, E., and Ramos, R.: Continuous quality assessment of atmospheric water vapour measurement techniques: FTIR, Cimel, MFRSR, GPS, and Vaisala RS92, Atmospheric Measurement Techniques, 3, 323–338, https://doi.org/10.5194/amt-3-323-2010, 2010.

Shaw, G. E.: Sun Photometry, Bulletin of the American Meteorological Society, 64, 4–10, https://doi.org/10.1175/1520-0477(1983)064<0004:SP>2.0.CO;2, 1983.

Shaw, G. E., Reagan, J. A., and Herman, B. M.: Investigations of Atmospheric Extinction Using Direct Solar Radiation Measurements Made with a Multiple Wavelength Radiometer, Journal of Applied Meteorology (1962-1982), 12, 374–380, 1973.

Silva Dias, M. A. F., Rutledge, S., Kabat, P., Silva Dias, P. L., Nobre, C., Fisch, G., Dolman, A. J., Zipser, E., Garstang, M., Manzi, A. O., Fuentes, J. D., Rocha, H. R., Marengo, J., Plana-Fattori, A., Sá, L. D. A., Alvalá, R. C. S., Andreae, M. O., Artaxo, P., Gielow, R., and Gatti, L.: Cloud and rain processes in a biosphere-atmosphere interaction context in the Amazon Region, Journal of Geophysical Research:Atmospheres, 107, LBA 39–1–LBA 39–18, https://doi.org/10.1029/2001JD000335, 8072, 2002.

Sinyuk, A., Holben, B. N., Smirnov, A., Eck, T. F., Slutsker, I., Schafer, J. S., Giles, D. M., and Sorokin, M.: Assessment of error in aerosol optical depth measured by AERONET due to aerosol forward scattering, Geophysical Research Letters, 39, n/a–n/a, https://doi.org/10.1029/2012GL053894, l23806, 2012.

Tomasi, C.; Petkov, B.H. Calculations of relative optical air masses for various aerosol types and minor gases in Arctic and Antarctic atmospheres. Journal of Geophysical Research: Atmospheres. 2014, 119, 1363–1385. https://doi.org/10.1002/2013JD020600

van Donkelaar, A., Martin, R. V., Brauer, M., Kahn, R., Levy, R., Verduzco, C., and Villeneuve, P. J.: Global Estimates of Ambient Fine Particulate Matter Concentrations from Satellite-Based Aerosol Optical Depth: Development and Application, Environmental Health Perspectives, 118, 2010.

van Donkelaar, A., Martin, R. V., Spurr, R. J. D., Drury, E., Remer, L. A., Levy, R. C., and Wang, J.: Optimal estimation for global ground-level fine particulate matter concentrations, Journal of Geophysical Research: Atmospheres, 118, 5621–5636, https://doi.org/10.1002/jgrd.50479, 2013.

Yamasoe, M. A. and do Rosario, N. E.: Changes in solar radiation partitioning reaching the surface due to biomass burning aerosol particles in the Amazon Basin, AIP Conference Proceedings, 1100, 657–660, https://doi.org/10.1063/1.3117072, 2009.

Yamasoe, M. A., Rosario, N. M. E. d., Leiva, E. A., Costa, T. S., and Braghiere, R. K.: Aerosol optical properties, downward solar irradiance and Ozone concentrations measured at Humaitá, AM, during the biomass burning season of 2012, in: In: Changing chemistry in a changing world: Scientific Program, International Commission on Atmospheric Chemistry and Global Pollution, 2014.